Micro-Grid Autonomous Operation During and Subsequent to Islanding Process

F. Katiraei, *Student Member, IEEE*, M. R. Iravani, *Fellow, IEEE*, and P. W. Lehn, *Member, IEEE*

***Abstract*—This paper investigates (i) preplanned switching events and (ii) fault events that lead to islanding of a distribution subsystem and formation of a micro-grid. The micro-grid includes two distributed generation (DG) units. One unit is a conventional rotating synchronous machine and the other is interfaced through a power electronic converter. The interface converter of the latter unit is equipped with independent real and reactive power control to minimize islanding transients and maintain both angle stability and voltage quality within the micro-grid. The studies are performed based on a digital computer simulation approach using the PSCAD/EMTDC software package. The studies show that an appropriate control strategy for the power electronically interfaced DG unit can ensure stability of the micro-grid and maintain voltage quality at designated buses, even during islanding transients. This paper concludes that presence of an electronically-interfaced DG unit makes the concept of micro-grid a technically viable option for further investigations.**

***Index Terms*—Distributed generation, distributed resources, electromagnetic transients, islanding, micro-grid, power sharing, voltage regulation.**

I. Introduction

DISTRIBUTED generation (DG) units, distributed storage (DS) units and integrated distributed generation/storage (DG+DS) units constitute the broader family of distributed energy resources (DR). Available and currently developing technologies for DG and DS units are based on i) combustion engines, micro- and mini-gas-turbines, wind turbines, fuel-cells, solar-thermal systems, photovoltaic systems, low-head hydro units and geothermal systems and ii) battery storage, capacitor storage, low- and high-speed flywheel systems and Superconducting Magnetic Energy Storage (SMES) systems. While only DG units are considered in this paper, many similarities exist between the operation of DG units and other DR units in terms of system studies. A DG unit may be interfaced to the grid either directly through an AC rotating machine or through a power electronic converter. A unit which utilizes a power electronic conversion system as the interfaced medium provides a higher degree of speed and flexibility to control the output frequency, voltage and real/reactive power of the unit.

Deregulation of the electric utility industry, environmental concerns associated with central electric power plants, volatility of electric energy cost, and rapid technological developments of DG systems all support the proliferation of DG units in electric utility systems. Furthermore, the increase in DG penetration depth and the presence of multiple DG units in electrical proximity to one another have brought about the concept of the micro-grid [1], [2]. A micro-grid is formed when an electrical region capable of autonomous operation is islanded from the remainder of the grid; e.g., a distribution substation along with its feeders that service both DG units and local loads. Formation of a micro-grid due to an islanding process can be due to disturbances, such as a fault and its subsequent switching incidents, or due to preplanned switching events. The micro-grid is to remain operational in an autonomous mode after islanding and meet the corresponding load requirements.

Current utility practices do not permit autonomous micro-grid operation and, except in special cases, require that all down stream DG units be disconnected after both planned or unplanned switching events. This requirement is imposed to address safety concerns and to comply with the existing control/protection constraints of distribution systems [3], [4]. However, to realize the full benefit of high DG penetration depth, the autonomous operation of micro-grids needs to be considered. Clearly, micro-grid operation has a far reaching impact on the existing safety, control, protection and dispatch practices and strategies of electrical energy, yet micro-grid operation has neither been fully understood nor investigated. The objectives of this paper are:

- To demonstrate typical electromagnetic transients of a micro-grid due to preplanned and unplanned switching incidents and the subsequent islanding process.
- To illustrate that a properly controlled DG unit which is interfaced to the micro-grid with a power electronic converter can minimize the impact of transients and maintain stability of the micro-grid.
- To highlight further areas for investigation.

To conduct the proposed studies, a study system is defined and the corresponding PSCAD/EMTDC based digital computer simulation model is developed. Section II of the paper introduces the study system. Section III discusses the islanding process and formation of a micro-grid. Section IV briefly deals with the islanding detection requirements. Section V describes the specifics of the PSCAD/EMTDC model of the study system. Results of the study and discussions are reported in Sections VI and VII respectively. Conclusions are stated in Section VIII.

II. Study System

Fig. 1 shows a single-line diagram of the system used to investigate typical micro-grid operational scenarios. The basic

Manuscript received March 11, 2003; revised May 31, 2003. Paper no. TPWRD-00103-2003.

The authors are with the Department of Electrical and Computer Engineering, University of Toronto, Toronto, ON M5S 3G4, Canada (e-mail: katiraei@ele.utoronto.ca; iravani@ecf.utoronto.ca; lehn@ecf.utoronto.ca).

Digital Object Identifier 10.1109/TPWRD.2004.835051

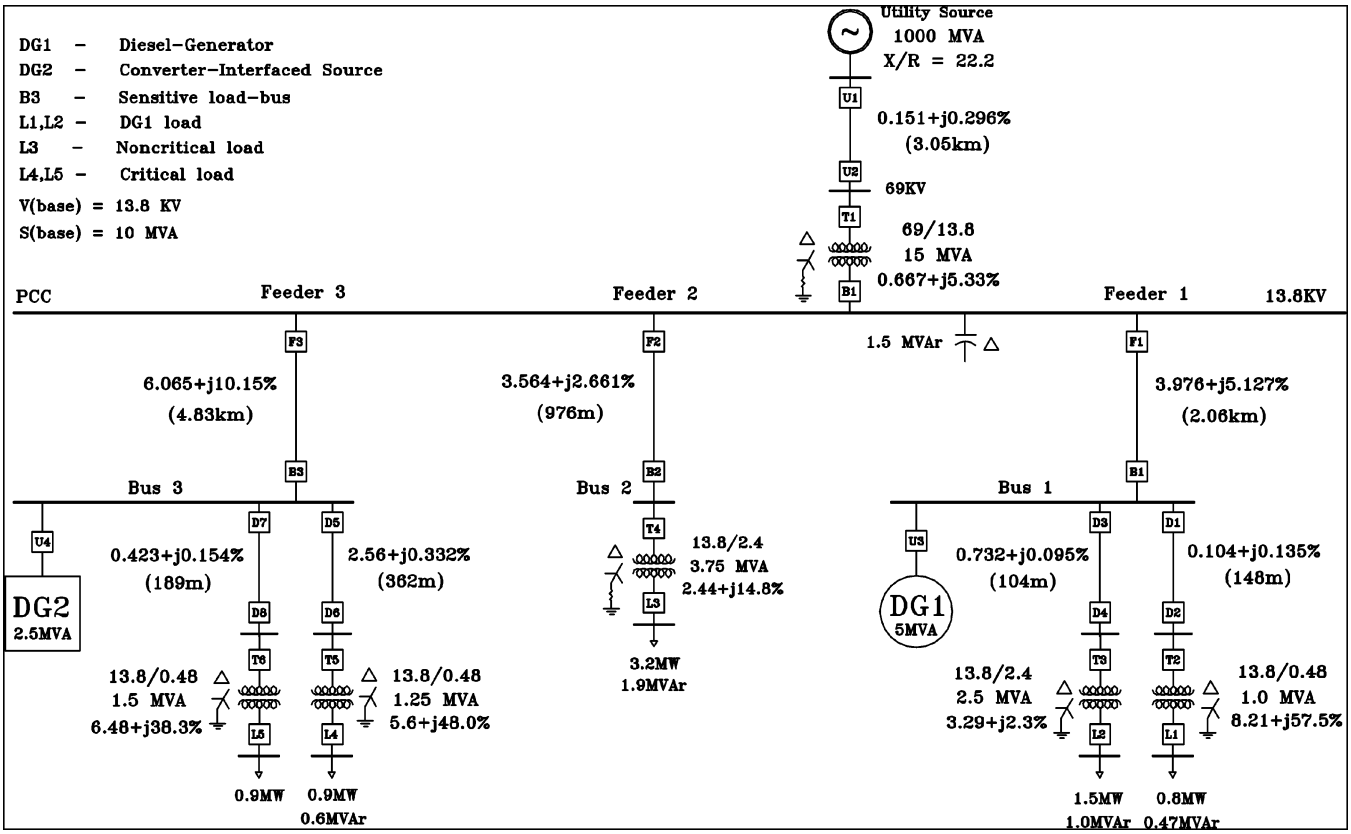

Fig. 1. Single-line diagram of the study system.

system configuration and parameters were extracted from the benchmark system of the IEEE Standard 399-1997 [5], with some modifications to allow for autonomous micro-grid operation. The system is composed of a 13.8-kV, three-feeder distribution subsystem which is connected to a large network through a 69-kV radial line. The 13.8-kV distribution substation is equipped with a three-phase 1.5-MVAr, fixed shunt-capacitor bank. The 13.8-kV substation busbar is radially connected to the main grid through the substation transformer and a 69-kV line. The network at the end of the 69-kV line is represented by a 69-kV, 1000-MVA short-circuit capacity bus. A combination of linear and nonlinear loads ($L1$ to $L5$) are supplied through three radial feeders of the subsystem. Loads $L1$ to $L4$ are composed of linear RL branches. Load $L5$ is a three-phase diode-rectifier load. The aggregate of $L4$ and $L5$ constitutes a sensitive load within the distribution subsystem.

The system also includes two DG units, i.e., $DG1$ (5-MVA) and $DG2$ (2.5-MVA) on feeders $F1$ and $F3$ respectively. $DG1$ is a synchronous rotating machine equipped with excitation and governor control systems. It may represent either a diesel-generator or a gas-turbine-generator unit. $DG2$ utilizes a voltage-sourced converter (VSC) as the interface medium between its source and the power system. $DG2$ represents a dispatchable source with adequate capacity to meet the real/reactive power commands, within pre-specified limits, subsequent to disturbances. Such a dispatchable source may also include energy storage interfaced at the converter dc bus. $DG2$ provides control on its output real and reactive power components independently.

III. Micro-Grid Formation Due to Islanding

A micro-grid is a portion of a power system which includes one or more DR units and is expected to remain operational after separation from the system. In the context of the study system of Fig. 1, the 13.8-kV distribution system, including the loads and the two DG units, constitutes the micro-grid.

The islanding phenomenon that results in the formation of a micro-grid can be due to either preplanned or unplanned switching incidents. In the case of a preplanned micro-grid formation, appropriate sharing of the micro-grid load amongst the DG units and the main grid may be scheduled prior to islanding. Thus, the islanding process results in minimal transients and the micro-grid continues operation, albeit as an autonomous system. Pre-planned islanding and subsequent micro-grid operation is discussed in [6]. In the context of this paper, a preplanned islanding of the 13.8-kV system can happen by scheduled opening of the circuit breakers at both ends of the 69-kV line, e.g., for line maintenance.

An unplanned islanding and micro-grid formation is due to either a fault and its subsequent switching incidents or some other unexpected switching process. Prior to islanding, the operating conditions of micro-grid could be widely varied, e.g., the DG units can share load in various manners and the entire micro-grid portion of the network may be delivering or importing power from the main grid. Furthermore, the disturbance can be initiated by any type of fault and line tripping may be followed up with single or even multiple reclosure actions. Thus, the severity of the transients experienced by the micro-grid, subsequent to

an unplanned islanding process, is highly dependent on i) the pre-islanding operating conditions, ii) the type and location of the fault that initiates the islanding process, iii) the islanding detection time interval, iv) the post-fault switching actions that are envisioned for the system and v) the type of DG units within the micro-grid. For the system of Fig. 1, an unplanned islanding scenario due to a fault on the 69-kV line followed by line tripping and both successful and unsuccessful reclosures are considered.

After islanding, reconnection of the micro-grid to the utility grid is permitted only once restoration of the main system and the micro-grid is achieved. Grid restoration is identified when system voltages and frequencies have returned to, and been maintained in, a normal range for a reasonable period of time, e.g., 5 minutes [7]. This reconnection must be carried out through proper synchronization of the micro-grid to the utility at the point of common coupling (PCC). Limits have been proposed for acceptable voltage magnitude error, frequency error and phase-angle error between the micro-grid and the main grid. For micro-grids with DG units in 1.5-MW to 10-MW range, reconnection is acceptable if voltage error is below 3%, frequency error below 0.1 Hz, and phase-angle error below 10° [7]. Adhering to these limits ensures reconnection of the micro-grid may be achieved with minimal transients in the overall system.

TABLE I
DISTRIBUTED GENERATIONS SPECIFICATION

DG1 Specifications S_b = 5 MVA , V_b = 13.8 kV			
Ra	0.0052 (p.u)	X_{ls}	0.2 (p.u)
X_d	2.86 (p.u)	X_q	2.0 (p.u)
X_d'	0.7 (p.u)	X_q'	0.85 (p.u)
X_d''	0.22 (p.u)	X_q''	0.2 (p.u)
T_{do}'	3.4 (s)	T_{do}''	0.01 (s)
T_{qo}''	0.05 (s)	H	2.9 (s)

DG2 Specifications	
Converter Structure	7-cell cascaded inverters
Rated Voltage	13.8 kV
Rated Power	2.5 MVA
Switching Frequency	1260 HZ
Tie Impedance (R_f + jX_f)	0.01 + j0.15 (p.u)

TABLE II
FEEDER LOADS AND REPRESENTING EQUIVALENT IMPEDANCES

	Maximum Power MW + MVAr	Equivalent Impedance (Ω)
Feeder 1	0.8 MW , 0.47 Mvar	176.91 + j 104.00
	1.5 MW , 1.0 Mvar	88.17 + j 58.48
Feeder 2	3.2 MW , 1.9 Mvar	48.25 + j 17.04
Feeder 3	0.9 MW , 0.6 Mvar	119.02 + j 104.95
	0.9 MW	Diode Rectifier + 386 Ω

IV. ISLANDING DETECTION AND PROTECTION

Under the present regulations governing distribution system operation, an islanding scenario is only permitted for loads with dedicated generation units. As a result, DG units must be equipped with specific islanding detection and prevention schemes to disconnect the unit within 2 seconds of an islanding event [7]. Several active and passive techniques have been introduced to detect an islanding condition, using local power system measurements [8]–[10]. In the case of future micro-grid applications, with the potential of autonomous operation, a fast and reliable detection algorithm is required to effectively distinguish between an islanding condition and other types of disturbances. In the studies reported here, the islanding and formation of a micro-grid is assumed to be detected within 2 to 5 cycles depending on the severity of the fault that initiates the process. After detection an autonomous micro-grid control strategy is activated.

After islanding auto reclosure action may reconnect the micro-grid to the main grid. Provisions must therefore also be made to detect a successful reclosure and re-activate the grid-connected control strategy of the micro-grid.

V. STUDY SYSTEM MODEL

To investigate the micro-grid operational scenarios, the PSCAD/EMTDC software package is used to develop a time domain simulation model of the study system of Fig. 1. The component models used for the simulation are as follows. The main grid is represented by a 69-kV three-phase voltage source with the short-circuit capacity of 1000 MVA and X/R ratio of 22.2. The 69-kV line is represented by a three-phase line with lumped, series RL elements per phase. The three-phase, triple-pole circuit breakers at both ends of the 69-kV line are modeled as ideal switches which can open at line current zero crossing instants. The substation 69/13.8-kV transformer and the load transformers are represented as linear, three-phase transformers with the appropriate winding connections, Fig. 1. Each feeder is represented as a three-phase overhead line or cable with lumped RL elements per phase. Loads $L1$ to $L4$ are modeled as three-phase, lumped, linear RL elements. Load $L5$ is modeled as a three-phase diode rectifier which feeds a resistive load at its dc side.

DG1 is modeled as a single-mass synchronous machine. The machine electrical system is represented in the d-q-0 frame with two rotor windings on each axis. The excitation and governor systems of the machine are also included in the model. $DG2$ is represented by a three-phase equivalent of a multi-level converter system. Each terminal of the converter is connected to the system through a lumped series RL branch. The control system of the converter is represented in the d-q-0 frame and utilizes the concept of instantaneous power to control real/reactive power exchange with the system by specifying d and q components of converter currents [11], [12]. The converter dc side is represented as a constant dc voltage source. The system parameters are given in Fig. 1, Tables I and II.

The simulation model also encompasses measurement circuitry; including frequency estimation block, angle tracking block and instantaneous real/reactive power measurement block. The frequency estimation block is implemented based on a cycle-to-cycle calculation of the time interval between two consecutive zero crossing of the voltage waveform. The angle tracking block provides a synchronization reference signal for interfacing the converter of $DG2$, independent of the variations in the frequency, during dynamic and steady state operating conditions. To measure real and reactive power generations of each DG unit and power transfer from the grid, instantaneous

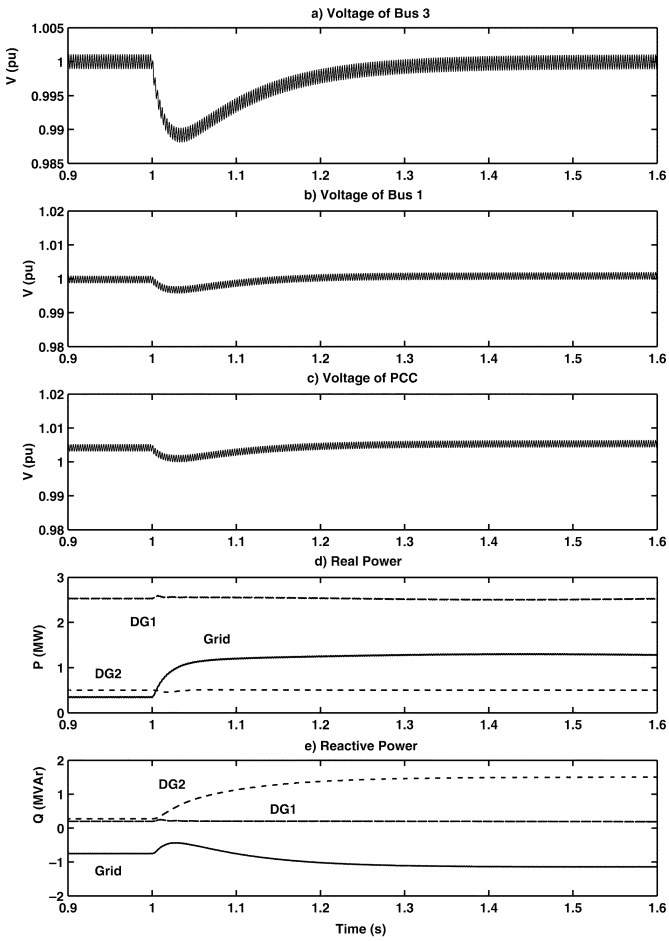

Fig. 2. Case(1)- L4 energization at $t = 1$ s.

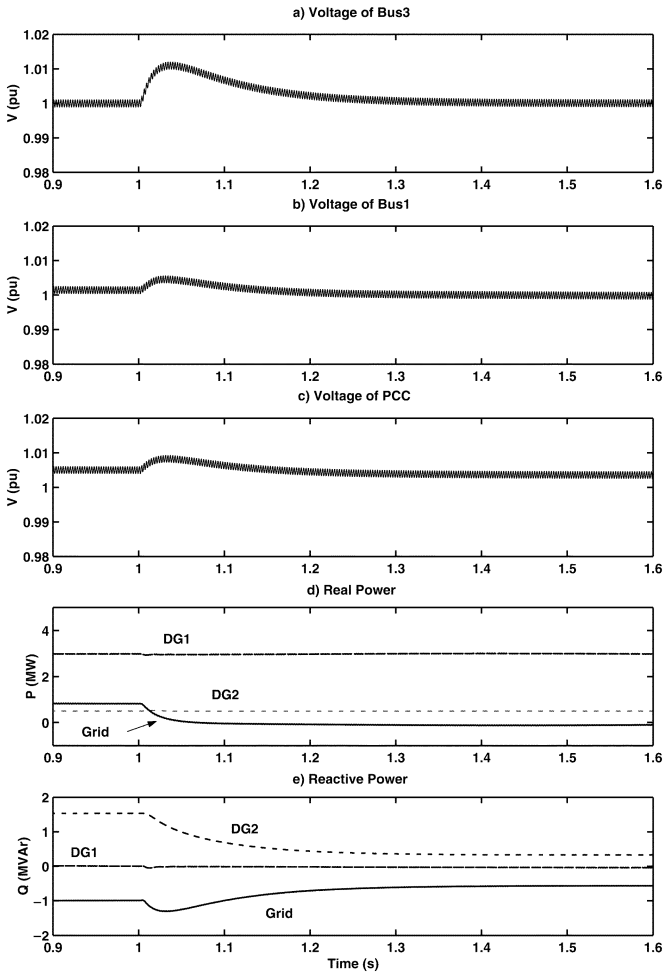

Fig. 3. Case(1)- L4 de-energization at $t = 1$ s.

values of corresponding three-phase bus voltages and line currents are measured and converted to the required quantities.

VI. Study Cases

Several case studies are conducted to examine the 13.8-kV system operation in grid-connected mode, during separation and in islanded mode. Case studies are chosen to illustrate both the steady state response to the changes in the system operating point, and the dynamic response when the system undergoes a transient.

Case (1): Grid-Connected Mode: The objective of this case study is to demonstrate that the VSC-based $DG2$ can be controlled to provide regulation of voltage and/or reactive power at its terminal to meet the requirement of the sensitive load $(L4 + L5)$ at bus 3, Fig. 1. In the grid-connected mode, real power outputs from $DG1$ and $DG2$ are set at pre-specified levels. Thus any change in power demand by loads $L1$ to $L5$ is accommodated by the main grid. Initially the total load is 3.2-MW and 1.77-MVAr of which 90% is supplied by $DG1$ and $DG2$ and the rest by the main grid. $L4$ is then energized at time $t = 1$ s. Fig. 2 illustrates the impact of $L4$ energization on the bus voltages and the power output of $DG1$, $DG2$ and the main grid. $DG2$, through the control of the q-component of converter current, adjusts its reactive power injection [11] to maintain the voltage at bus 3; even though this results in injecting reactive power into the main grid. Fig. 2 shows that the sensitive load voltage, bus 3, is maintained within $\pm 1\%$. Fig. 2(d) also indicates that based on the adopted strategy, the real power of $L4$ is fully supplied by the grid. $DG2$ only adjusts its injected reactive power to maintain the bus voltage.

Fig. 3 shows the impact of disconnecting (de-energization) $L4$ on the system voltages and power flows. Prior to de-energization, 81% of the load is supplied by DG units and the rest imported from the main grid. After $L4$ de-energization, $DG2$ maintains the corresponding bus voltage through reactive power control and the excessive real power generated by DG units is exported to the main grid, Fig. 3.

It should be noted that in the above two scenarios, $DG2$ can also be controlled to rapidly adjust its real power in addition to its reactive power, if it is required.

Case (2): Pre-Planned Islanding: The objective of this study is to investigate transient behavior of the micro-grid due to a preplanned islanding scenario. Prior to islanding, $DG1$ and $DG2$ supply 3.0-MW and 0.5-MW respectively to the local load, i.e., 88% of the total load, and the rest is imported from the main grid. At $t = 0.8$ s a preplanned islanding command is issued to the 69-kV line breakers, and the real power set point of $DG2$ is changed from 0.5 to 1.5-MW. $DG1$, through the action of its governor, adjusts itself to supply the rest of the micro-grid real power demand according to its dynamic response time. $DG2$

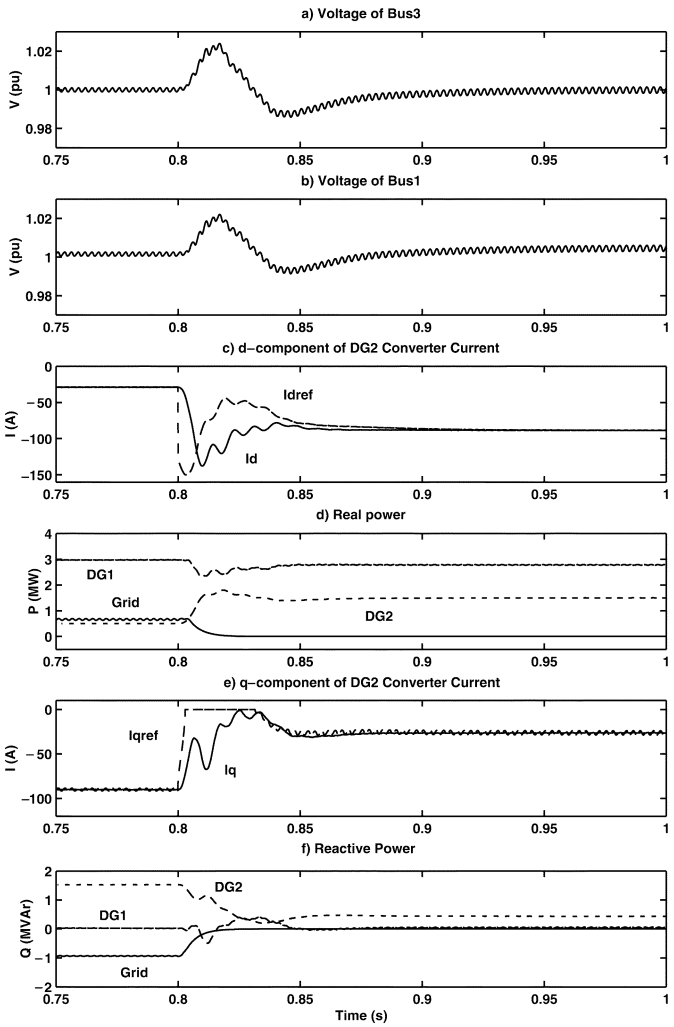

Fig. 4. Case(2)- Pre-planned islanding at $t = 0.8$ s.

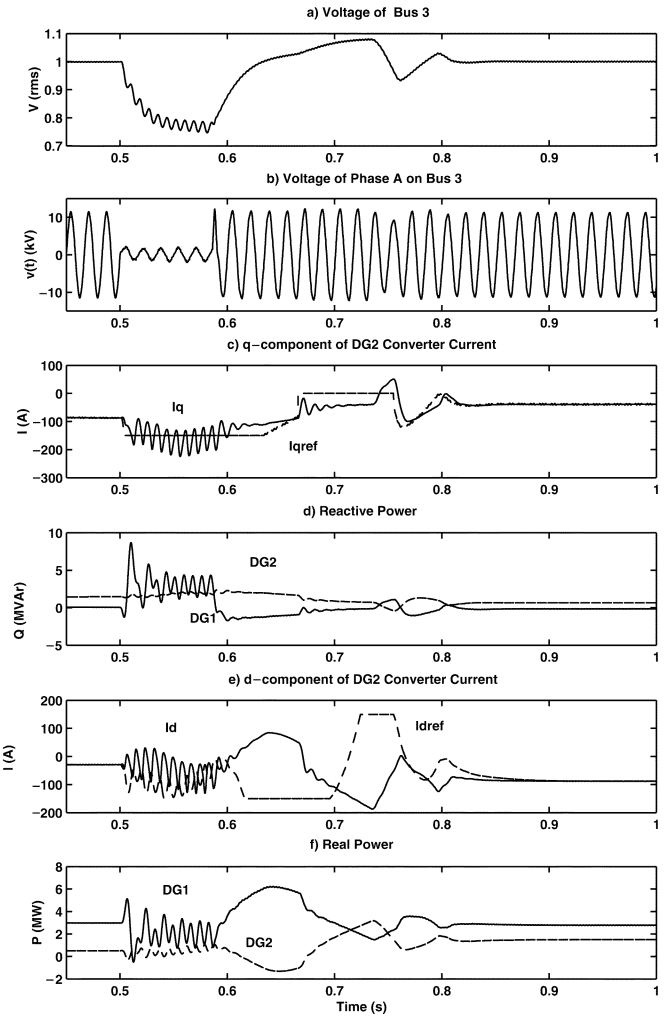

Fig. 5. Case (3a): L-G fault at $t = 0.5$ s, CB's opening at $t = 0.583$ s, islanding detection at $t = 0.666$ s.

also controls its injected reactive power to maintain the voltage at bus 3. Fig. 4 shows the system transients due to the planned islanding. Fig. 4 shows that variations of the voltage at bus 3 is less than 2%. Fig. 4 also shows power sharing of the DG units after islanding, where the response times of the real/reactive power controllers are less than 50 ms. The frequency change in the micro-grid, due to the islanding process, is limited between 59.80 Hz to 60.55 Hz and then settles to 60 Hz. The study results indicate that the micro-grid can maintain the desired power quality, even for the sensitive load, during the preplanned islanding transients.

Case (3a): Line to Ground $(L$-$G)$ Fault:

a) Temporary L-G Fault: A L-G fault occurs on the 69-kV line at $t = 0.5$ s. The fault is cleared by triple-pole operation of CB's at both ends of the line, 5 cycles after the fault inception, e.g., at $t = 0.583$ s, and a micro-grid is formed due to the accidental islanding. The islanding phenomenon is detected 5 cycles after the CB's open, e.g., at $t = 0.666$ s, at which time the micro-grid control strategy of the DG units is activated whereby the real power set point of $DG2$ is changed from 0.5 to 1.5-MW. Prior to the fault, power delivered by $DG1$, $DG2$ and the utility are 3-MW/0.1-MVAr, 0.5-MW/1.5-MVAr and 0.85-MW/1.0-MVAr, respectively. Fig. 5 shows the transients during the fault, fault clearing, separation and islanding detection. During the fault, voltage severely drops [Fig. 5(a) and (b)] and the reactive power control of $DG2$ reaches its limit [Fig. 5(c) and (d)] to inject the maximum reactive power in the system. Upon clearing the fault, control actions in $DG1$ and $DG2$ eventually return the voltage to its normal range. Transiently, however, due to the limited reactive power injection ability of $DG2$ and the field time constant of $DG1$, large voltage variations [Fig. 5(a) and (b)] cannot be prevented. Fig. 5(d) and (f) also show power sharing between $DG1$ and $DG2$ after the fault. Fast control action of $DG2$ maintains the new power levels for both DG units in less than 200 ms.

The CB's of the 69-kV line employ triple-pole auto-reclosure and attempt to re-connect the micro-grid to the main grid 30 cycles after the fault clearing, i.e., $t = 1.083$ s. Since the fault is temporary and clears before reclosure, the reclosure is successful. Fig. 6 shows the system transients due to the reclosure. After reclosure, the control reference for the delivered power of $DG2$ is kept unchanged and its reactive power is controlled to regulate the voltage on the sensitive load bus.

From the fault inception instant to the reclosure instant, the voltages of the micro-grid may drift with respect to that of the main grid, as shown in Fig. 7. Thus the reclosure is equivalent to

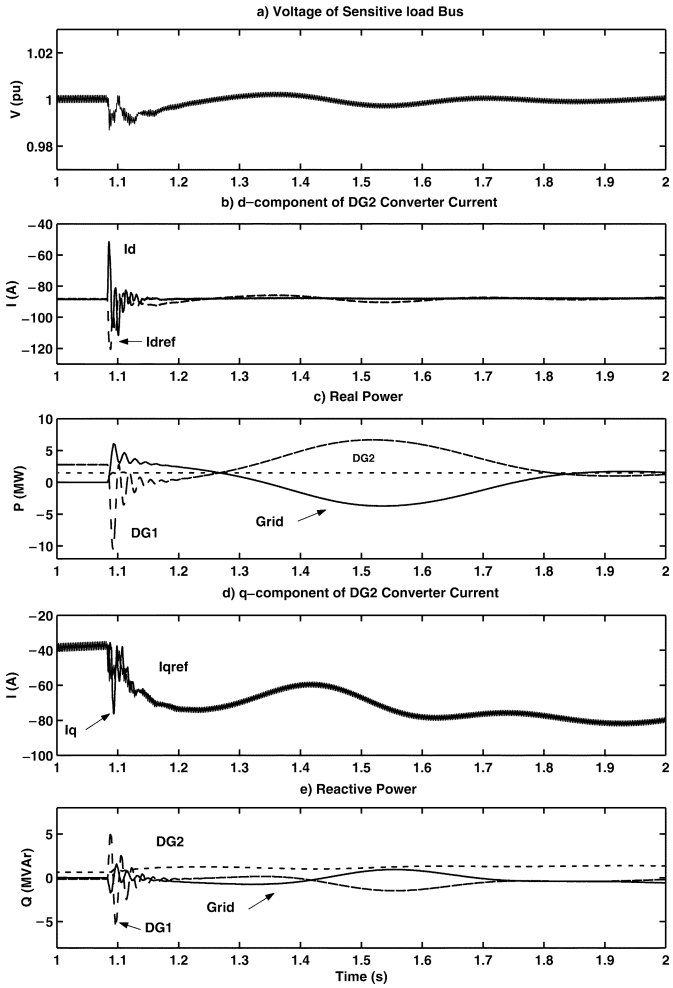

Fig. 6. Case (3a): Successful reclosure at $t = 1.083$ s.

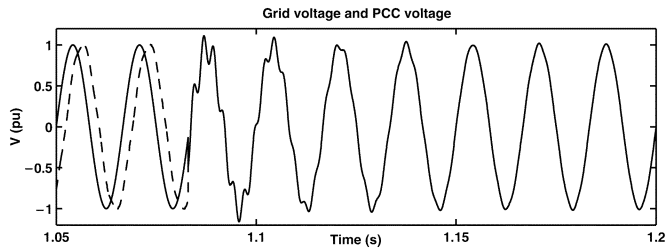

Fig. 7. Case (3a): Successful reclosure at $t = 1.083$ s.

a mal-synchronization of the micro-grid with respect to the main grid. This out-of-phase synchronization results in large swings of $DG1$, Fig. 8. This case study shows that the fast control action of $DG2$ attenuates the transients imposed on the micro-grid, maintains stability of $DG1$, and consequently ensures continuity of supply for the loads within the micro-grid.

b) Permanent L-G Fault: For this case study, the pre-fault operating conditions, control settings and the fault are the same as the previous case, except that the fault is permanent. Therefore, the micro-grid behavior up to the instant of reclosure is identical to that of the previous case. Due to the permanent nature of the fault, the reclosure at $t = 1.083$ s is unsuccessful and subjects the micro-grid to the second L-G fault which is cleared after 5 cycles, i.e., at $t = 1.166$ s. The system permits three

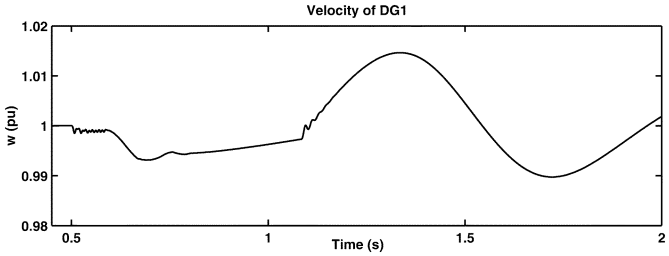

Fig. 8. Case (3a): L-G fault at $t = 0.5$ s, CB's opening at $t = 0.583$ s, islanding detection at $t = 0.666$ s, successful reclosure at $t = 1.083$ s.

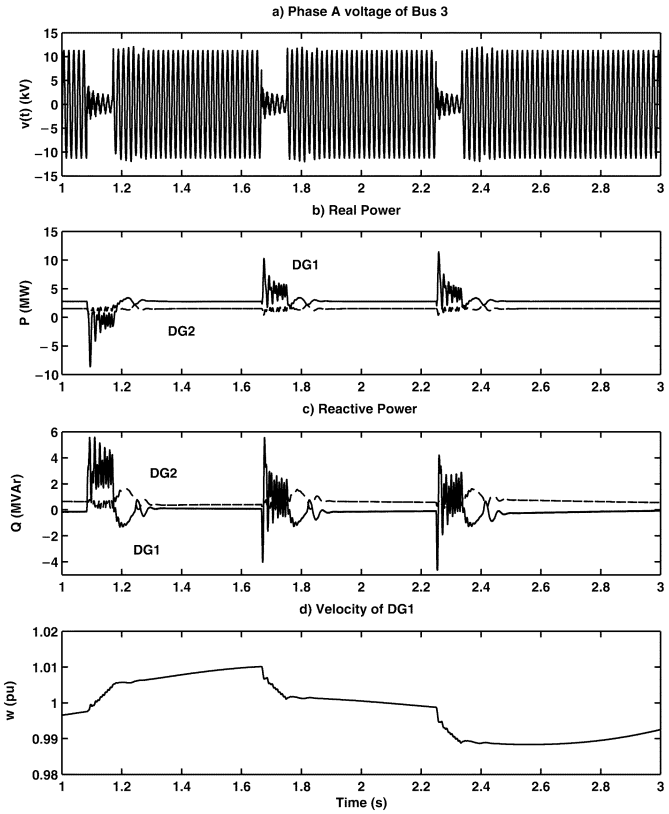

Fig. 9. Case (3a): Three unsuccessful reclosure attempts subsequent to the permanent L-G fault.

subsequent unsuccessful reclosure attempts and then keeps the 69-kV CB's open until the utility system is restored and then manual reconnection permitted.

After each unsuccessful reclosure, the subsequent reclosure is attempted after another 30 cycles. After the third unsuccessful reclosure attempt and the corresponding fault clearing, the micro-grid continues its permanent operation as an autonomous system. Fig. 9 shows the micro-grid transients due to the three unsuccessful reclosures. Fig. 9(a) shows that except during the short-circuit (fault) time intervals, the reactive power control strategy of $DG2$ maintains the voltage of bus 3 within an acceptable range. During the first unsuccessful reclosure, power demand from $DG1$ decreases [Fig. 9(b)] and consequently its rotor accelerates [Fig. 9(d)]. However, during the next two unsuccessful reclosures the real power demand increases [Fig. 9(b)] and leads to the deceleration of $DG1$ [Fig. 9(d)].

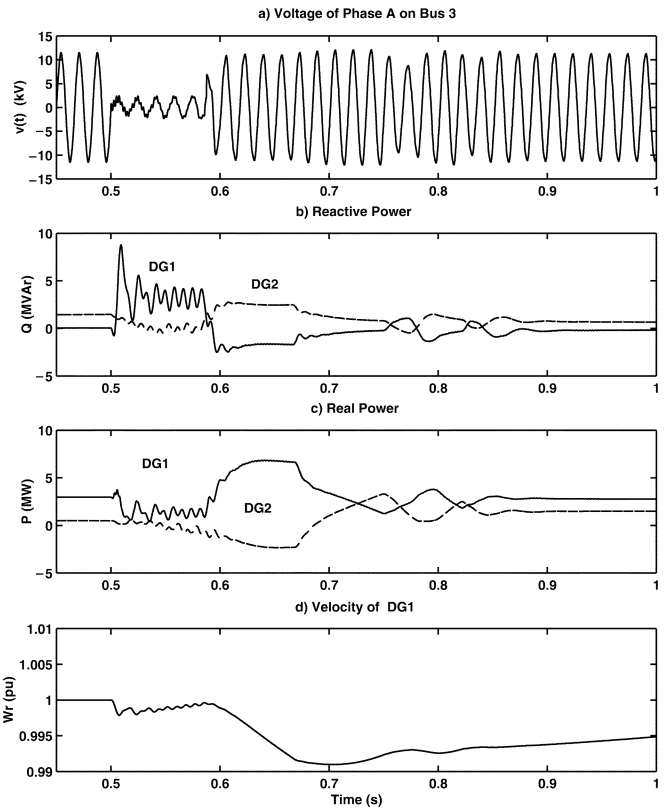

Fig. 10. Case (3b): L-L fault at $t = 0.5$ s, CB's opening at $t = 0.583$ s, islanding detection at $t = 0.666$ s.

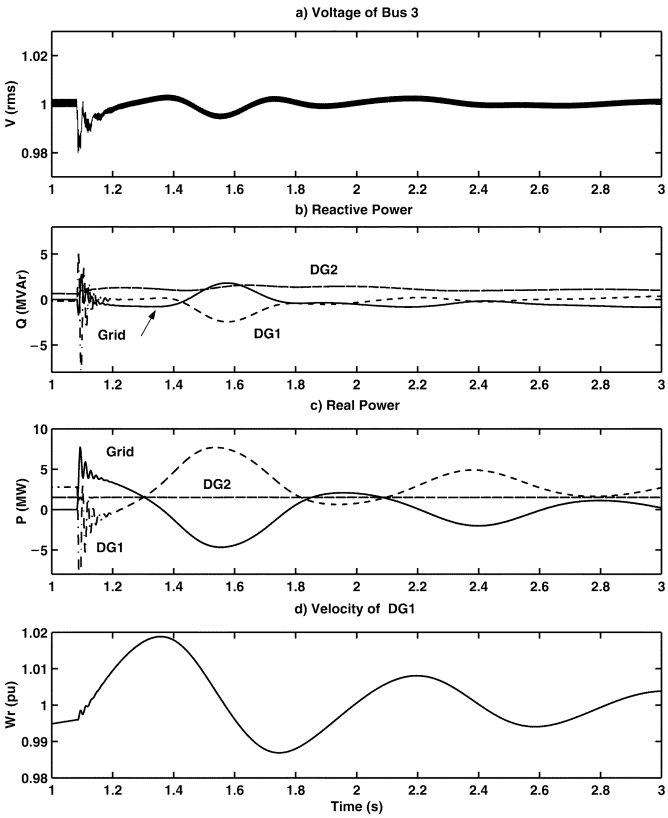

Fig. 11. Case (3b): Successful reclosure at $t = 1.083$ s.

The control strategy and the fast response of $DG2$ maintain the stability of the micro-grid and reduces impacts of the faults and the subsequent unsuccessful reclosures.

Case (3b): Line-to-Line $(L$-$L)$ Fault:

a) Temporary L-L Fault: For this disturbance scenario a L-L fault is imposed on the 69-kV line instead of a L-G fault. The pre- and post-fault control strategy and pre-disturbance operating point are the same as those described for Case (3a)-a. Fig. 10 shows transients during the fault, fault clearing and islanding detection. Fig. 11 illustrates the bus 3 voltage transients and power swing between the utility grid and $DG1$ after the successful reclosure at $t = 1.083$ s.

Figs. 10 and 11 illustrate that real/reactive control strategy and fast response of $DG2$ maintain the stability and voltage quality (at bus 3) of the micro-grid and permits transition from grid-connected to micro-grid mode without load/generation shedding. Without the $DG2$ control action, the disturbance resulted in poor voltage quality or angle instability of the micro-grid as it illustrated in Appendix I.

b) Permanent L-L Fault: This case study is identical to the previous case except that the L-L fault is permanent and thus after three unsuccessful reclosures, the micro-grid is permanently formed and continues operation as an autonomous system. Study results for the three unsuccessful reclosure attempts are illustrated in Fig. 12. The results indicate that the proposed control strategy for $DG1$ and $DG2$ can effectively bring the micro-grid to a steady state operating point and minimize transients as a result of the fault and its subsequent disturbances.

Similar to the case of a permanent L-G fault, the $DG2$ control action can maintain stability of the micro-grid after the permanent L-L fault. The voltage magnitude, except during fault intervals, is also well regulated by reactive power control of $DG2$.

Case (3c): Three-Phase Line-to-Ground $(L$-L-L-$G)$ Fault: This case study investigates the micro-grid formation and its electrical transients due to a permanent L-L-L-G fault on the 69-kV line. The time intervals corresponding to fault clearing, islanding detection and reclosure attempts are the same as those of the previous case studies except that system islanding is detected in 2 cycles (as opposed to 5 cycles in the previous cases). Islanding detection in 2 cycles is possible in this case because of the severe voltage drop due to the L-L-L-G fault. Fig. 13 shows the system transients prior to the first reclosure attempt. Fig. 14 shows the transients due to three unsuccessful reclosures.

Although this fault scenario subjects the system to four subsequent bolted, three-phase faults, the proposed control strategy of $DG2$ ensures angle stability and voltage recovery of the micro-grid. The case studies reported in Appendix I show that the micro-grid $(DG1)$ loses angle stability without the control action of $DG2$.

VII. Discussion

Prior to discussing the case study results, the scope of this investigation must be re-clarified. First, the proposed micro-grid is assumed to be balanced, i.e., no single-phase loads or unbalanced three-phase loads are considered. Secondly, the two DG units within the micro-grid, due to their noticeably different time constants, do not exhibit any dynamic interactions

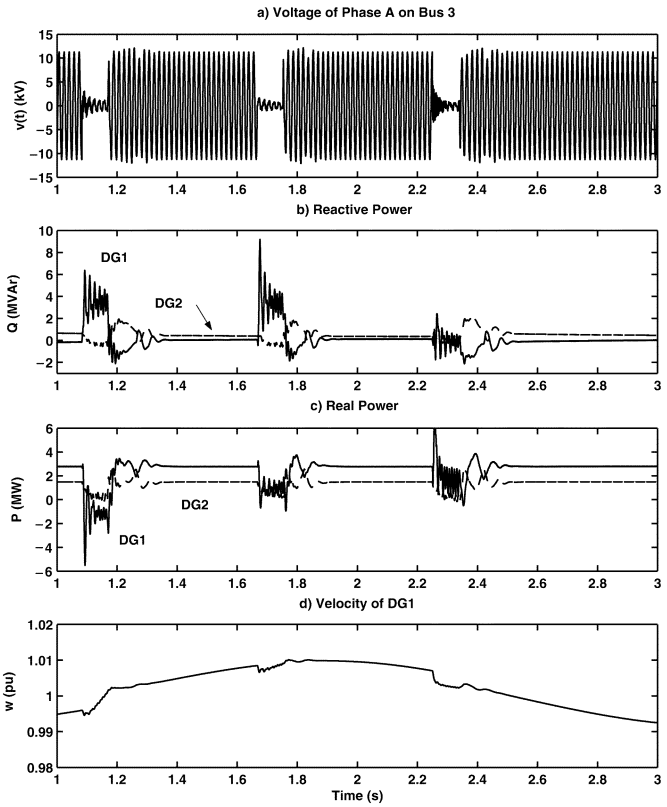

Fig. 12. Case (3b): Three unsuccessful reclosure attempts subsequent to the permanent L-L fault.

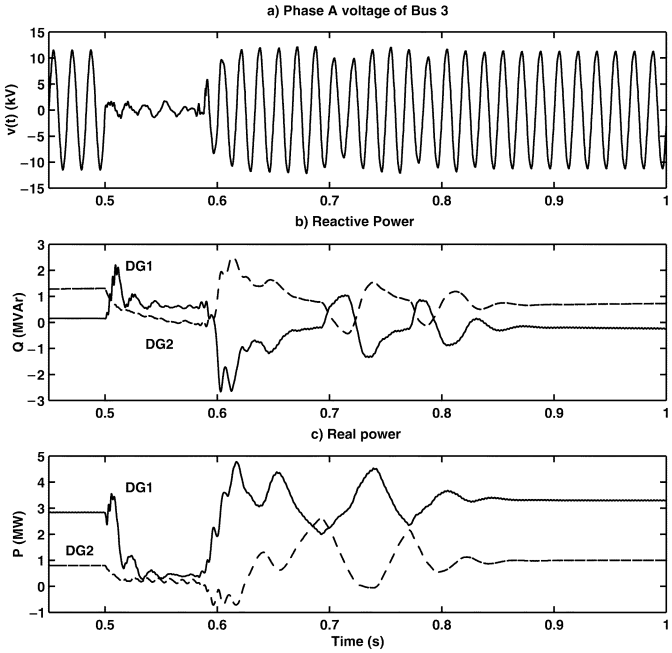

Fig. 13. Case (3c): L-L-L-G fault at $t = 0.5$ s, CB's opening at $t = 0.583$ s, islanding detection at $t = 0.666$ s.

during transients. In case of multiple converter-interfaced DG units, dynamic interactions may occur among units. Such interactions are not addressed in this paper. Thirdly, transient overvoltages/overcurrents and the corresponding control/protection issues and methods are not discussed in this paper.

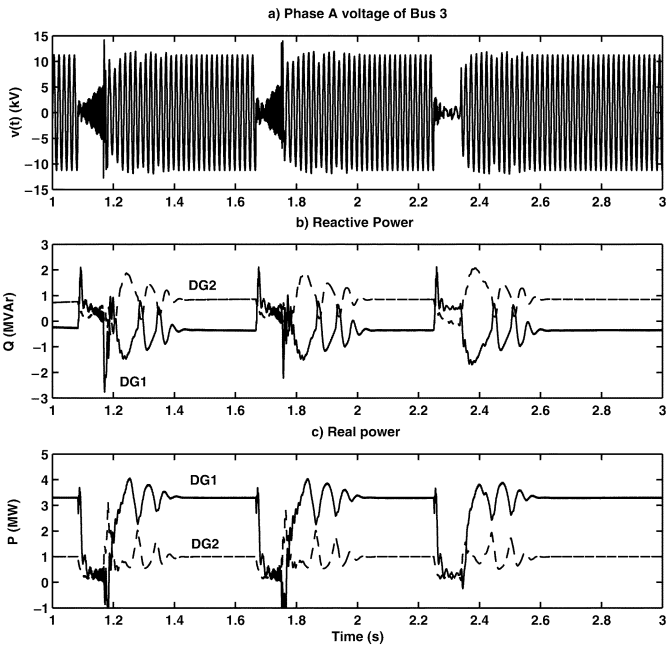

Fig. 14. Case (3c): Three unsuccessful reclosure attempts subsequent to the permanent L-L-L-G fault.

The following conclusions can be drawn based on the conducted case studies.

- During grid connected mode, the micro-grid operating strategy is determined according to load requirements and the available capacity of DG units. Normally, variations in load demand are primarily supplied by the utility grid, with DG units possibly modifying their output through the application of new power generation set points. As a result, DG units can be controlled to adequately contribute to voltage regulation or reactive power compensation of the sensitive load bus, where fast real power support is not the top concern.
- In case of preplanned islanding, micro-grid DG set points are adjusted for autonomous operation prior to islanding. Transfer into islanded mode may thereby be achieved with minimal transients. The study indicates that the micro-grid can maintain the desired power quality, even for the sensitive load, during the preplanned islanding transitions.
- Fault studies verify that successful transfer into autonomous micro-grid operation may be achieved under the investigated fault scenarios. Successful transfer does, however, require islanding detection and a subsequent change in control strategy of micro-grid DG units.
- Simulation results illustrate that reclosure after a temporary fault is feasible. Successful reclosure depends on the reclosing time interval, where the maximum allowable drift in the phase angle difference between the micro-grid voltage and the main grid voltage at the PCC limits the time of reclosing.
- In case of a permanent fault occurrence, automatic line reclosing results in reconnection of both the utility and the micro-grid to the faulted line. Although successful transfer to autonomous islanded operation of the micro-grid will eventually result, transiently the system undergoes severe

disturbances due to the unsuccessful reclosure attempts. The reclosure attempts cause large currents to flow out of the micro-grid and into the fault, resulting in severely depressed micro-grid bus voltages. However, the adopted control strategy ensures angle stability and voltage recovery of the micro-grid and consequently ensures continuity of supply for the loads within the micro-grid.

- For all scenarios, disturbances result in system frequency variations and power swings within the micro-grid. The fast control action of the converter interfaced DG unit can effectively damp such oscillations.
- It should be noted that the controllers of the DG units of the study system are not optimized. Therefore, better performance than illustrated can be achieved.
- In the fault scenarios, the fault has zero impedance and is imposed on the system on the 69-kV line, in close proximity to the 13.8/69-kV transformer. Thus, the micro-grid is exposed to the most severe faults in terms of fault impedance and location. Consequently, a better performance can be expected under less severe transient conditions.

VIII. Conclusion

This paper investigates various islanding scenarios of a 13.8-kV distribution system from the main grid and its autonomous operation as a micro-grid. The micro-grid is supplied by two distributed generation (DG) units, i.e., a synchronous machine and an electronically interfaced DG unit. The former DG unit is equipped with excitation and governor controls and the latter unit includes fast, independent real and reactive power controls. The simulation studies show that the latter unit:

i) can maintain angle stability of the micro-grid even after most severe islanding transients, primarily through its fast real power control, and

ii) can enhance voltage quality at specific buses, mainly through its fast reactive power control.

Without the fast control of the electronically interfaced DG unit, the micro-grid experiences angle instability subsequent to islanding and its autonomous operation is not possible. The studies also demonstrate that through the fast control of the DG units, the concept of micro-grid formation and its autonomous operation are technically viable and merit further in-depth investigation.

Several issues which require further investigation in the context of micro-grid are: i) islanding detection and verification, ii) protection strategies and relay coordination to prevent unwanted equipment tripping during and subsequent to islanding process, iii) development of control strategies/algorithms for multiple electronically interfaced DGs to achieve optimum response in terms of voltage/angle stability, iv) evaluation of transient overcurrents/overvoltages due to islanding process in the micro-grid and provisions for countermeasures, v) investigation of voltage quality of sensitive loads of micro-grid subsequent to islanding process, vi) impact of single-phase and unbalanced loads on the control, protection and behavior of the micro-grid and vii) utilization of communications for coordinated control of DG units within the micro-grid.

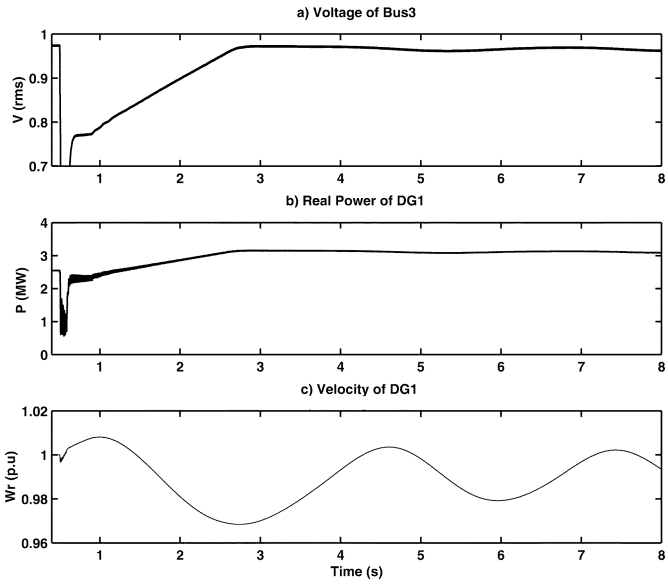

Fig. 15. L-L fault at $t = 0.5$ s, CB's opening at $t = 0.583$ s, $DG2$ not in service.

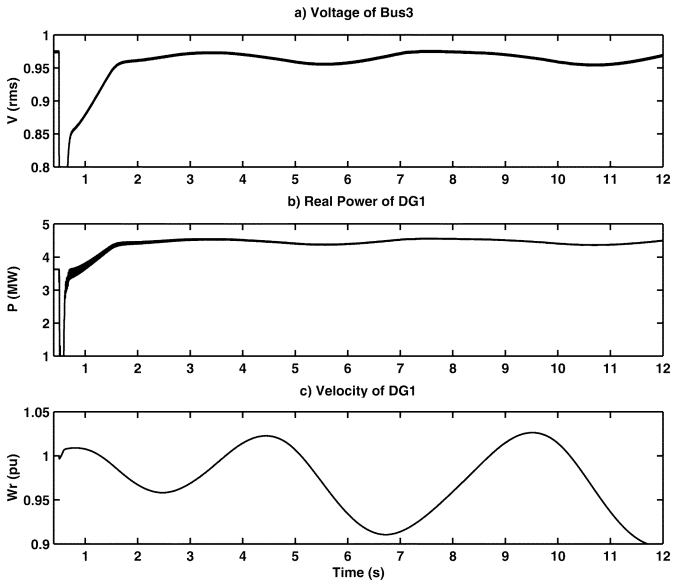

Fig. 16. L-L-L-G fault at $t = 0.5$ s, CB's opening at $t = 0.583$ s, $DG2$ not in service.

Appendix

The purpose of this appendix is to demonstrate that without the fast response of $DG2$, the micro-grid may fail to maintain voltage quality and/or angle stability subsequent to some islanding cases.

Fig. 15 shows the system transient response subsequent to islanding due to a L-L fault at $t = 0.5$ s which results in islanding at $t = 0.583$ s. Prior to the fault the total system load is 3.3-MW, $DG2$ is disconnected and $DG1$ is in service. Fig. 15 shows that subsequent to the islanding process, $DG1$ adjusts its output to meet the load demand and the system assumes a new stable operating point. However, due to the slow response of $DG1$, voltage at the sensitive bus, Bus 3, does not meet the ITI requirements [13] for tens of cycles, Fig. 15(a). Presence of $DG2$ in service

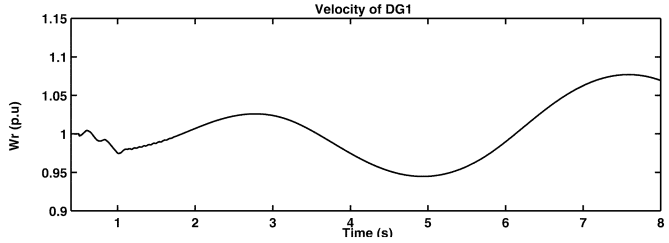

Fig. 17. L-L-L-G fault at $t = 0.5$ s, CB's opening at $t = 0.583$ s and real power control of $DG2$ is activated with the delay of $t = 0.5$ s.

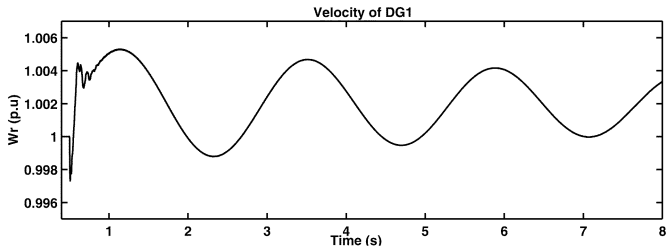

Fig. 18. L-L-L-G fault at $t = 0.5$ s, CB's opening at $t = 0.583$ s and real power control of $DG2$ is activated with 2-cycle delay.

would have maintained the voltage at Bus 3 within a few cycles after the islanding process, Figs. 10(a) and 12(a).

Fig. 16 shows the system behavior due to a L-L-L-G fault at $t = 0.5$ s followed by an islanding process at $t = 0.583$ s. Prior to the fault, the load demand is 4.3-MW/2.4-MVAr from which 1.5-MVAr is supplied by the capacitor bank. $DG2$ is disconnected and $DG1$ is in service. Fig. 16 demonstrates that due to the islanding process $DG2$ experiences oscillations and finally loses angle stability, Fig. 16(c), although the load demand is below its rated power capacity.

It should be mentioned that the presence of an electronically-interfaced DG unit does not guarantee angle stability of the system. Instead, angle stability will require sufficiently fast response of the real power control associated with $DG2$. Fig. 17 shows speed variations of $DG1$ due to the same L-L-L-G disturbance scenario when the real power control of DG2 is activated 500 ms after islanding. Fig. 17, similar to Fig. 16(c), demonstrates that the micro-grid still experiences angle instability due to slow response of $DG2$. Fig. 18, in contrast, shows speed variations of $DG1$ for the same disturbance scenario when the real power control of $DG2$ is activated 2 cycles after the islanding. Fig. 18 indicates that the micro-grid retains angle stability.

Comparison of Figs. 16(c)–18 clearly demonstrate the impact of the fast response of $DG2$ on maintaining angle stability of the micro-grid.

REFERENCES

[1] N. D. Hatziargyriou and A. P. S. Meliopoulos, "Distributed energy sources: Technical challenges," in *Proc. IEEE Power Eng. Soc. Winter Meeting*, vol. 2, New York, 2002, pp. 1017–1022.

[2] C. L. Smallwood, "Distributed generation in autonomous and nonautonomous micro grids," in *Proc. Rural Electric Power Conf.*, 2002, pp. D1–D1-6.

[3] A. P. S. Meliopoulos, "Challenges in simulation and design of microgrids," in *Proc. IEEE Power Eng. Soc. Winter Meeting*, vol. 1, New York, 2002, pp. 309–314.

[4] R. C. Dugan, "Distributed resources and reliability of distribution systems," in *Proc. IEEE Power Eng. Soc. Summer Meeting*, vol. 1, July 2002, pp. 105–108.

[5] *IEEE Recommended Practice for Industrial and Commercial Power System Analysis*, IEEE Std. 399-1997.

[6] P. Piagi and R. H. Lasseter, "Industrial Application of MiroGrids," Power System Engineering Research Center, Univ. Wisconsin, Madison, WI, 2001.

[7] *IEEE Draft Standard for Interconnecting Distributed Resources With Electric Power Systems*, IEEE WG Std. IEEE Std. 1547-2003, July 2001.

[8] M. A. Redfern and O. Usta, "Protection against loss of utility grid supply for a dispersed storage and generation unit," *IEEE Trans. Pow. Delivery*, vol. 8, pp. 948–954, July 1993.

[9] J. E. Kim and J. S. Hwang, *Islanding Detection Method of Distributed Generation Units Connected to Power Distribution System*: Power Syst. Technol., 2000, vol. 2, pp. 643–647.

[10] F. S. Pai and S. J. Huang, "A detection algorithm for islanding-prevention of dispersed consumer-owned storage and generating units," *IEEE Trans. Energy Conversion*, vol. 16, pp. 346–351, Dec. 2001.

[11] C. Schauder and H. Mehta, "Vector analysis and control of the advanced static VAR compensators," *Proc. Inst. Elect. Eng. C*, vol. 140, no. 4, pp. 299–306, July 1993.

[12] R. H. Lasseter, "Microgrid," in *Proc. IEEE Power Emg. Soc. Winter Meeting*, vol. 1, New York, 2002, pp. 305–308.

[13] R. C. Dugan and M. F. McGranaghan, *Electrical Power Systems Quality*, 2nd ed. New York: McGraw-Hill, 2002, pp. 41–42.

F. Katiraei (S'01) received the B.Sc. and M.Sc. degrees in electrical engineering from Isfahan University of Technology, Isfahan, Iran, in 1995 and 1998, respectively. He is currently pursuing the Ph.D. degree at the University of Toronto, Toronto, ON, Canada.

M. R. Iravani (F'03) received the B.Sc. degree in electrical engineering from Tehran Polytechnique University, Tehran, Iran, in 1976, and the M.Sc. and Ph.D. degrees in electrical engineering from the University of Manitoba, Winnipeg, MB, Canada, in 1981 and 1985, respectively.

Currently, he is a Professor at the University of Toronto, Toronto, ON, Canada. His research interests include power electronics and power system dynamics and control.

P. W. Lehn (M'99) received the B.Sc. and M.Sc. degrees in electrical engineering from the University of Manitoba, Winnipeg, MB, Canada, in 1990 and 1992, respectively, and the Ph.D. degree from the University of Toronto, Toronto, ON, Canada, in 1999.

Currently, he is an Assistant Professor with the University of Toronto. From 1992 to 1994, he was with the Network Planning Group of Siemens AG, Erlangen, Germany.